DIRECT INTERFACING OF NEURONS TO HIGHLY INTEGRATED MICROSYSTEMS

Andreas Hierlemann
ETH Zurich, Department of Biosystems Science and Engineering
CH-4058, Basel, Switzerland

ABSTRACT

The use of large high-density transducer arrays enables fundamentally new neuroscientific insights through enabling high-throughput monitoring of action potentials of larger neuronal networks (> 1000 neurons) over extended time to see effects of disturbances or developmental effects, and through facilitating detailed investigations of neuronal signaling characteristics at subcellular level, for example, the study of axonal signal propagation that has been largely inaccessible to established methods. Applications include research in neural diseases and pharmacology.

INTRODUCTION

To understand how functions and characteristics of neuronal networks arise from the concerted interactions of the involved neurons, it is necessary to have methods that allow for interacting with neuronal functional subunits and ensembles - somas, axons, dendrites, single neurons, as well as entire networks - at high spatiotemporal resolution and in real time [1-4]. Electrical recordings are among the oldest techniques [3-7].

Extracellular electrical recordings by means of microtransducer arrays complement well-established patch clamp techniques [6, 7] and optical or optogenetic techniques [8-11]. Commercially available standard MEAs (circuitless and passive) are an established technology for recording from networks of neurons [12-15]. However, due to their limited spatial resolution (pitch > 30 μm) and limited number of electrodes (< 300), such circuitless MEAs typically do neither allow for recording details of targeted individual neurons nor for monitoring large networks.

High-density MEAs (HD-MEAs) offer the potential to simultaneously record from a large number of sites at high spatiotemporal resolution and in different frequency bands (action-potential (AP) and local-field potential (LFP) band) to obtain information on the properties of individual cells or neurons and on the dynamics in neuronal networks. Each electrode can also be used to locally stimulate [4, 16-18]. Simultaneous recordings of multiple neurons are tedious to realize by patch-clamp, and the cells are only viable for a short time [19, 20]. Optical and optogenetic methods provide multi-unit recording and stimulation over extended times, yet still have limited temporal resolution, and it is difficult to detect or to stimulate single action potentials (APs) in individual cells due to stray light and light scattering [3, 9-11].

CMOS HIGH-DENSITY SYSTEMS

CMOS (complementary metal oxide semiconductor) technology-based planar, high-density microelectrode arrays (HD-MEAs) feature several thousands of transducers at densities of > 3'000 transducers per mm^2 [4, 18, 21-26] (Figure 1), which enables recordings from large neuronal networks at single-cell, or even subcellular-component resolution [27, 28]. The integrated systems feature tightly-spaced transducers and the respective addressing and read-out circuitry on a single chip [4, 21-26].

Several different approaches relying on metal electrodes or open-gate field-effect transistors (FETs), as schematically shown in Fig. 1a, have been pursued [21, 22, 24, 26]. In the case of open-gate FET transducers, additional stimulation spots are needed and distributed between the electrodes. A sensor site and the surrounding stimulation site can be seen in Fig. 1b

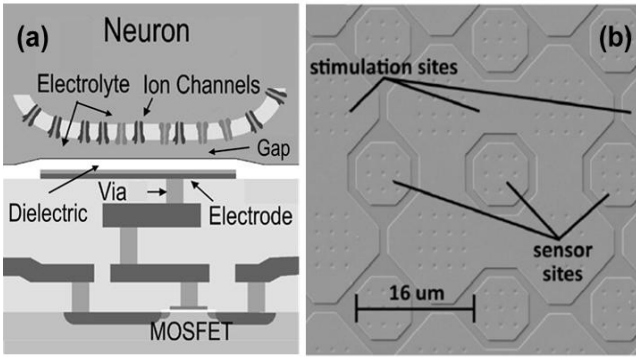

Figure 1: CMOS realization of an open-gate field-effect transistor array. (a) Schematic cross section of a CMOS chip; the transistor gate is connected via several metal layers and vias to an electrode on top of the chip, which is covered by a dielectric material, such as high-k Ti-Zr oxide. Adapted from [21]. (b) Chip surface of a fabricated CMOS-based HD-MEA based on open-gate FETs. The much larger stimulation site completely surrounds the sensor site in the center [24].

Besides the comparably large, planar *in-vitro* systems, which are in the focus of this contribution, there are also CMOS-based needle-type probes for recording and stimulation *in vivo* that have been pioneered at the University of Michigan [3, 29-33] and adopted by other groups (Figure 2) [34-37]. Such electrode arrays are inserted into the living brain and facilitate advances in the understanding of the nervous system. Merged with on-chip circuitry, signal processing, microfluidics, and wireless interfaces, they are forming the basis for a family of neural prostheses for the possible treatment of disorders, such as blindness, deafness, paralysis, severe epilepsy, and Parkinson's disease [31].

The use of CMOS helps to overcome the connectivity problem of how to interface thousands of tightly-spaced transducers through provision of addressing and multiplexing units [4, 18, 26]. The use of

CMOS also helps to improve signal-to-noise characteristics, as signal conditioning is done on chip next to where the partially very small signals (< 10 µV) are generated. Using CMOS devices, local field potentials (LFPs), i.e., collective electrical activity of many neurons, have been recorded in brain slices, action potentials have been detected in dissociated neuronal cultures and brain slices, or various types of retinal ganglia have been identified [23, 38-43].

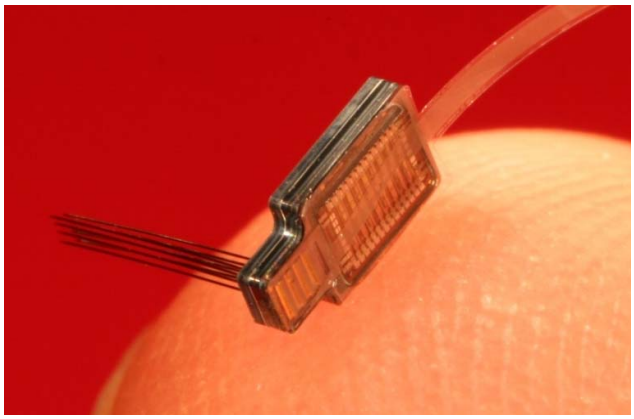

Figure 2: Very compact integrated neural recording microsystem frontend on an index finger featuring 64 electrodes: 4 electrodes per shank and 4 chips with 4 shanks each. At the right the cable connection can be seen [29, 30].

A disadvantage of CMOS chips is that silicon is not transparent to visible light in contrast to standard cell culture substrates used in biology. Additionally, the chip or its components can corrode upon operation and long-term exposure to liquids (salt water). Therefore, a good packaging solution is needed, on the one hand, to protect the chip against metabolic products and chemicals of the cell culture, and, on the other hand, to prevent the cells from being poisoned or disturbed by toxic materials released by the chip, such as the CMOS metals aluminum or copper that dissolve in saline solution.

In this contribution, we will demonstrate how highly integrated CMOS microelectrode array systems featuring several thousands of transducers (> 3'000 transducers per mm^2) can be used to record from or stimulate potentially any individual neuron or subcellular compartment on a CMOS chip [4, 21, 26, 28].

As one example, we show in Fig. 3 a HD-MEA system featuring a sensing area of 3.85 × 2.10 mm^2 hosting 26'400 Pt electrodes of 7 µm diameter at a center-to-center pitch of 17.5 µm [26, 28]. The switch matrix allows for simultaneously routing user-configurable selections of electrodes to 1024 recording channels with 10-bit 20-kS/s A/D conversion and 32 stimulation units at the array periphery. The readout channels provide programmable bandwidth and gain up to 78.3 dB. The integrated noise voltage of the full readout chain is 2.4 μV_{rms} in the action-potential (AP) signal band (300 Hz–10 kHz). The switch matrix can be reprogrammed within 1.4 ms to adapt to the morphology of the biological sample. Possible configurations include single electrodes, sets of electrodes at points of interest, or multiple contiguous high-density blocks of up to 23×23 electrodes.

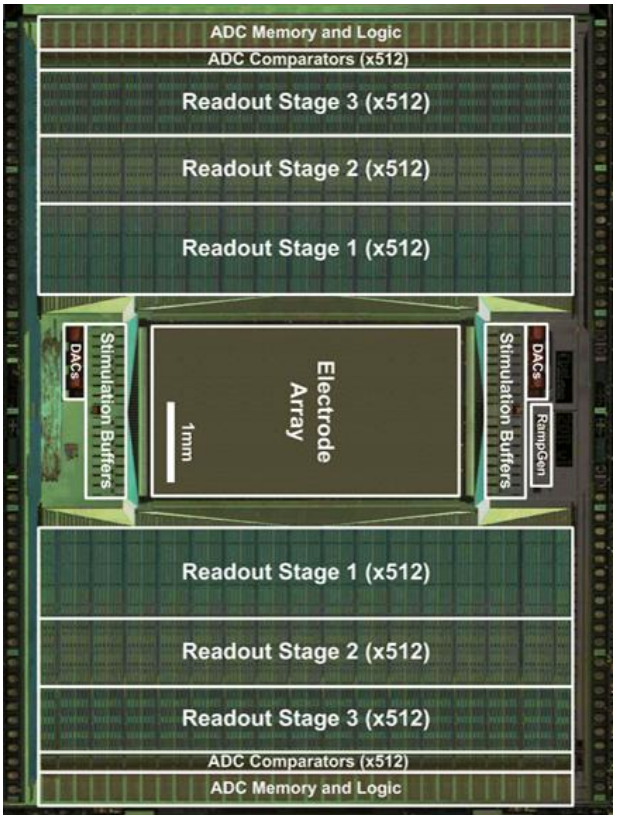

Figure 3: CMOS-based bidirectional HD-MEA system. 26'400 metal electrodes (Pt) at the center of the chip (3.85 x 2.1 mm^2) are surrounded by readout, stimulation, and addressing circuitry units (scale bar: 1 mm) [26].

MEASUREMENTS AND RESULTS

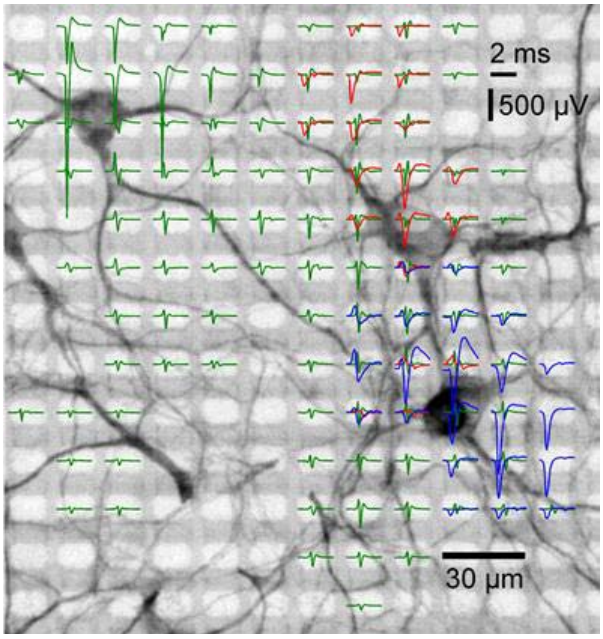

Figure 4: Electrical signals of 3 neurons, recorded by the HD-MEA at full resolution and superimposed to a fluorescence image of the cell culture (MAP2 staining). Spike-triggered signal averages (50 trials) in green (top left neuron), red (top right) and blue (bottom right) for each electrode site (rounded white rectangles). Only signals exceeding 50 µV are displayed for clarity [28].

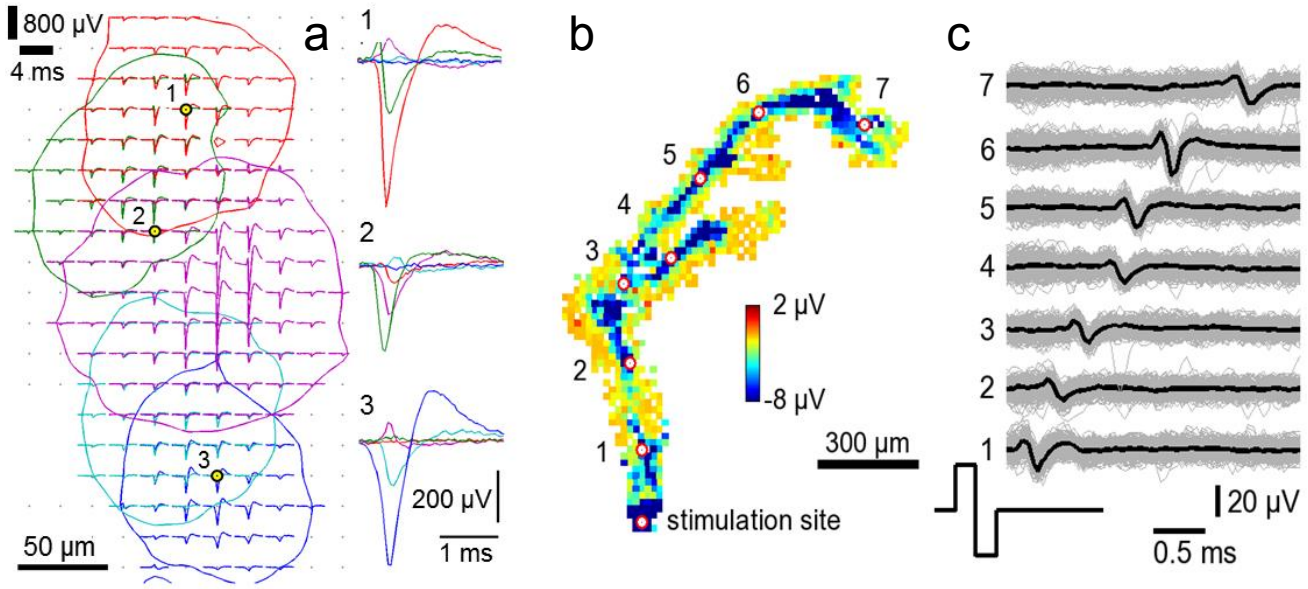

Figure 5: (a): High-resolution zoom-in on a small colony of neurons in a network. Five identified neurons with overlapping electrical footprints were obtained from all 209 electrodes in the area. Black-yellow circles indicate the 3 electrodes providing best separation of the signals of these 5 neurons, the respective spike-triggered average waveforms are given at the right [28]. (b-c): Axonal signals across a branching point recorded by simultaneously using 841 electrodes. (b): "Electrical image" of the axonal signals (rat cortical neurons at DIV 18). (c): Waveforms of the action potentials traveling along the axon as recorded from the electrodes marked in red on the center map. Typical axonal signal characteristics are observed: triphasic, first-positive signal [28].

With this system it was possible to record subcellular-resolution data in various preparations. Figure 4 shows the electrical signals of 3 neurons, recorded by the HD-MEA at full resolution and superimposed to a fluorescence image of the cell culture (MAP2-staining). The signals of three neurons, as obtained from the respective electrode sites (rounded white rectangles), are displayed in green (top left neuron), red (top right) and blue (bottom right). Figure 5 shows in the left panel a high-resolution zoom-in on a small colony of neurons in a network. From both figures it is evident that many electrodes always record from the same neuron and that every electrode simultaneously records activity of several neurons.

It was also possible to detect small signals of action potentials traveling along thin axons (~100 nm diameter) as shown in Figure 5 center and right panels [27, 28]. Axonal signals across a branching point were recorded by simultaneously using 841 electrodes. The action potential waveforms that have been recorded from the electrodes marked in red in Fig. 5 center panel are shown in the right panel. Typical axonal signal characteristics are observed: tri-phasic, first-positive signals [27, 28]. The grey lines represent individual signal traces, the black line the spike-triggered average signal.

Additionally, CMOS microtransducer arrays and integrated microsystems offer the capability to bi-directionally interact, also in closed loop and real time, with potentially every single neuron in a given neuronal network [17, 27, 44]. We investigated the relationship between stimulation location and reliability of neuronal responses to high-frequency threshold stimulations. To verify that classified signals matched neuronal morphology, we superimposed spike-triggered average footprints and micrographs of lipofected neurons (Fig. 6a) [44]. We produced excitability profiles and defined stimulation thresholds for the respective electrodes.

Neuron-wide stimulation over a range of voltages revealed the spatial distribution of sites with low thresholds for extracellular stimulation. The stimulation site featuring the lowest threshold typically was found within the center region of the neuron's spike-triggered average footprint (Fig. 6). The stimulation threshold was defined as the minimal voltage that triggered an AP on the readout electrodes in 100% of the trials. Stimulation was applied at 4 Hz for voltages from ±10 to ±1,000 mV, with steps of ±10 mV. The stimulation frequency of 4Hz was selected as it is, on the one hand, not high enough to affect the reliability of neuronal responses, but, on the other hand, sufficiently high to allow for consecutive stimulation of hundreds of electrodes within 2 hours.

We found that stimulation of the most sensitive site provided selective single-cell neuronal activation in 96 % of the cases when voltages at threshold values were applied. "Selective" in this context means that only the targeted neurons were activated. We performed stimulation-triggered recordings to construct stimulation maps (example in Fig. 6b) and excitability profiles (example in Fig. 6c) for 52 different neurons in 27 preparations. For all neurons, 1-3 sites had steep excitability profiles with remarkably low activation thresholds (example in Fig. 6c: electrodes 1, 2, 3), and the most sensitive sites typically resided near the peak of the AP footprints (example in Fig. 6b, electrode 1). In general, activation thresholds of the most sensitive sites had values between ~±30 and ~±90 mV.

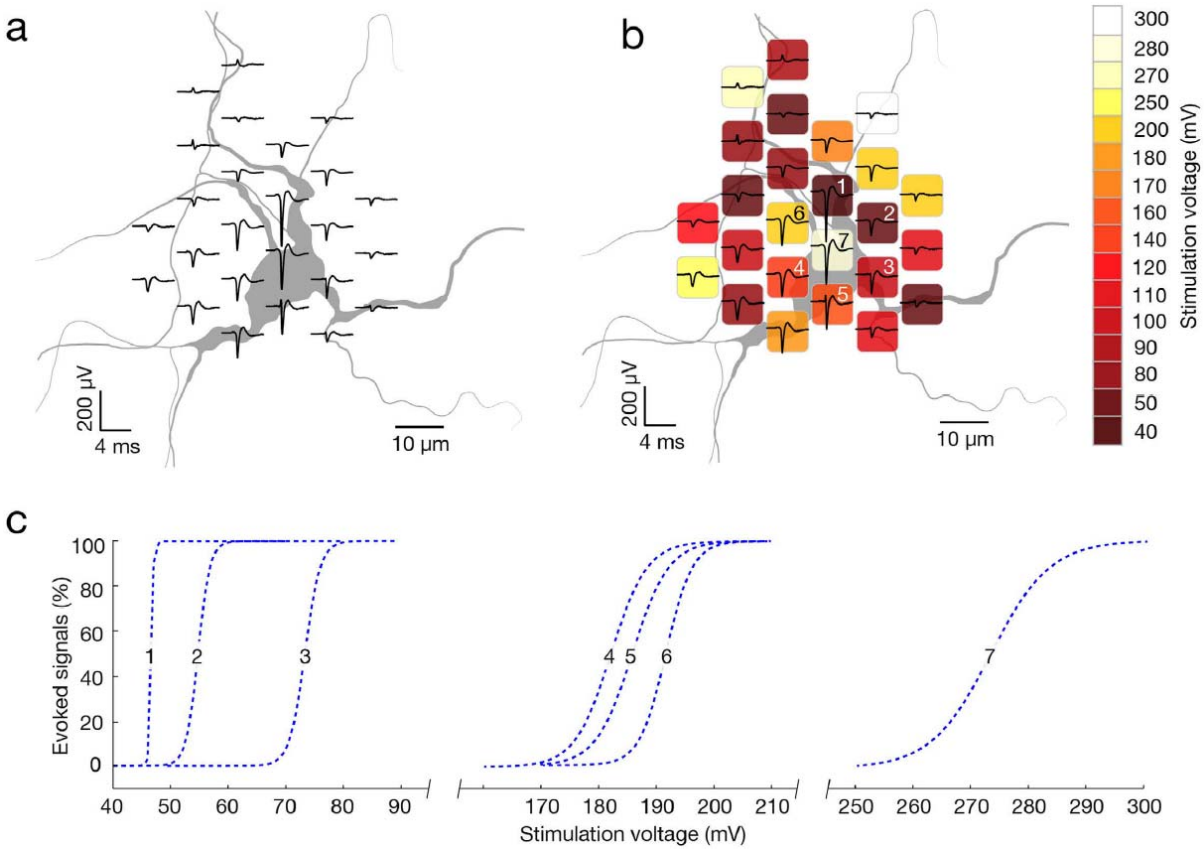

Figure 6: Selective stimulation of single neurons [44]. (a) Spontaneous activity footprint (black traces) superimposed over the morphology of the respective neuron and its proximal compartments (colored in gray). Neuronal morphology was inferred from a microscopy image of the lipofected neuron. (b) Stimulation map superimposed over the footprint and neuron morphology (same neuron as in A). Site-specific stimulation thresholds are color-coded, and the electrodes in the center of the spontaneous activity footprint are numbered (1-7). (c) Excitability profiles for stimulation through the 7 center electrodes. Numbers correspond to those in (b) [44].

OUTLOOK

Since neuronal signal transmission is (electro-)chemical, and since local fluctuations of ion concentrations, as well as anisotropic and inhomogeneous electrical conductivity of tissue and culture medium are critically influencing electric interaction with neurons, the next development step includes a multi-function high-density MEA system [45]. This monolithic system incorporates a large high-density electrode array of 2.43 × 4.48mm^2 including 59'760 electrodes at 13.5µm pitch (5'487 electrodes/mm^2) to record from large preparations/networks at subcellular resolution. Moreover it includes different functional circuitry units: 2048 action-potential readout channels featuring low noise levels of 3.2 μV_{RMS} (300 Hz to 10 kHz) to retrieve, for example, tiny axonal signals, 32 local-field-potential readout channels, 16 dual-mode voltage/current stimulation units, 32 impedance units, 28 neurotransmitter measurement units, and 32 current recording units. Separate AP and LFP recording units allow for improving specific amplifier characteristics without increasing overall readout unit complexity.

The system architecture also made use of the switch-matrix approach, as the intention was to deliver every system function to any arbitrarily selectable electrode/electrode sets to perform, at the same time, stimulation and measurements of various cell or network parameters in parallel. It was and is not feasible to repeat the various functional circuitry units within each pixel.

ACKNOWLEDGEMENTS

The intense work of all group members, several generations of PostDocs and PhD students working on CMOS design, microsystem post-processing, signal evaluation and analysis, and on carrying out the neuroscientific measurements is thankfully acknowledged. The work was financially supported by FP7 and H2020 of the European Union through the ERC Advanced Grants "NeuroCMOS" (AdG 267351) and "neuroXscales" (AdG 694829), and by the Swiss National Science Foundation through Grant 205321_157092/1 ("Axons") and the Sinergia grant CRSII3_141801.

REFERENCES

[1] A. P. Alivisatos, A. M. Andrews, E. S. Boyden *et al.*, "Nanotools for neuroscience and brain activity mapping," *ACS nano,* vol. 7, no. 3, pp. 1850-1866, 2013.

[2] A. H. Marblestone, B. M. Zamft, Y. G. Maguire *et al.*, "Physical principles for scalable neural recording," *Frontiers in computational neuroscience,* vol. 7, 2013.

[3] G. Buzsaki, E. Stark, A. Berenyi *et al.*, "Tools for Probing Local Circuits: High-Density Silicon Probes

Combined with Optogenetics," *Neuron,* vol. 86, no. 1, pp. 92-105, Apr, 2015.
[4] M. E. J. Obien, K. Deligkaris, T. Bullmann *et al.*, "Revealing neuronal function through microelectrode array recordings," *Frontiers in Neuroscience,* vol. 8, Jan, 2015.
[5] G. Buzsaki, "Large-scale recording of neuronal ensembles," *Nat Neurosci,* vol. 7, pp. 446-451, May, 2004.
[6] E. Neher, and B. Sakmann, "Single-channel currents recorded from membrane of denervated frog muscle fibres," *Nature,* vol. 260, no. 5554, pp. 799-802, Apr 29, 1976.
[7] K. S. Cole, "Dynamic electrical characteristics of the squid axon membrane," *Arch. Sci. physiol.,* vol. 3, pp. 253-258, 1949.
[8] D. R. Hochbaum, Y. Zhao, S. L. Farhi *et al.*, "All-optical electrophysiology in mammalian neurons using engineered microbial rhodopsins," *Nat Methods,* vol. 11, no. 8, pp. 825-33, Aug, 2014.
[9] M. Scanziani, and M. Häusser, "Electrophysiology in the age of light.," *Nature,* vol. 461, pp. 930-9, 2009.
[10] D. S. Peterka, H. Takahashi, and R. Yuste, "Imaging voltage in neurons," *Neuron,* vol. 69, no. 1, pp. 9-21, Jan 13, 2011.
[11] C. Grienberger, and A. Konnerth, "Imaging calcium in neurons," *Neuron,* vol. 73, no. 5, pp. 862-85, Mar 8, 2012.
[12] G. W. Gross, B. K. Rhoades, H. M. E. Azzazy *et al.*, "The use of neuronal networks on multielectrode arrays as biosensors," *Biosens. Bioelectron.,* vol. 10, pp. 553-567, 1995.
[13] A. Stett, U. Egert, E. Guenther *et al.*, "Biological application of microelectrode arrays in drug discovery and basic research," *Analytical and Bioanalytical Chemistry,* vol. V377, pp. 486-495, October, 2003.
[14] W. L. C. Rutten, "Selective electrical interfaces with the nervous system," *Annual Review Of Biomedical Engineering,* vol. 4, pp. 407-452, 2002.
[15] Y. Jimbo, and H. P. C. Robinson, "Propagation of spontaneous synchronized activity in cortical slice cultures recorded by planar electrode arrays," *Bioelectrochemistry,* vol. 51, pp. 107-115, June, 2000.
[16] S. Hafizovic, F. Heer, T. Ugniwenko *et al.*, "A CMOS-based Microelectrode Array for Interaction with Neuronal Cultures," *Journal of Neuroscience Methods,* vol. 164, no. 1, pp. 93-106, 2007.
[17] J. Muller, D. J. Bakkum, and A. Hierlemann, "Sub-millisecond closed-loop feedback stimulation between arbitrary sets of individual neurons," *Front Neural Circuits,* vol. 6, pp. 121, 2012.
[18] A. Hierlemann, U. Frey, S. Hafizovic *et al.*, "Growing Cells Atop Microelectronic Chips: Interfacing Electrogenic Cells In Vitro With CMOS-Based Microelectrode Arrays," *Proceedings of the IEEE,* vol. 99, no. 2, pp. 252-284, Feb, 2011.
[19] R. Perin, T. K. Berger, and H. Markram, "A synaptic organizing principle for cortical neuronal groups.," *Proceedings of the National Academy of Sciences of the United States of America,* vol. 108, pp. 5419-24, 2011.
[20] X. Jiang, G. Wang, A. J. Lee *et al.*, "The organization of two new cortical interneuronal circuits.," *Nature neuroscience,* vol. 16, pp. 210-8, 2013.
[21] B. Eversmann, M. Jenkner, F. Hofmann *et al.*, "A 128 x 128 CMOS biosensor array for extracellular recording of neural activity," *IEEE Journal of Solid-State Circuits,* vol. 38, pp. 2306-2317, 2003.
[22] L. Berdondini, K. Imfeld, A. Maccione *et al.*, "Active pixel sensor array for high spatio-temporal resolution electrophysiological recordings from single cell to large scale neuronal networks," *Lab on a Chip,* vol. 9, no. 18, pp. 2644-2651, 2009.
[23] G. Zeck, A. Lambacher, and P. Fromherz, "Axonal transmission in the retina introduces a small dispersion of relative timing in the ganglion cell population response," *PLoS ONE,* vol. 6, no. 6, pp. e20810, 2011.
[24] G. Bertotti, D. Velychko, N. Dodel *et al.*, "A CMOS-based sensor array for in-vitro neural tissue interfacing with 4225 recording sites and 1024 stimulation sites." pp. 304-307.
[25] U. Frey, J. Sedivy, F. Heer *et al.*, "Switch-Matrix-Based High-Density Microelectrode Array in CMOS Technology," *Journal of Solid-State Circuits, IEEE* vol. 45 no. 2, 2010.
[26] M. Ballini, J. Muller, P. Livi *et al.*, "A 1024-Channel CMOS Microelectrode Array With 26,400 Electrodes for Recording and Stimulation of Electrogenic Cells In Vitro," *Solid-State Circuits, IEEE Journal of,* vol. 49, no. 11, pp. 2705-2719, 2014.
[27] D. J. Bakkum, U. Frey, M. Radivojevic *et al.*, "Tracking axonal action potential propagation on a high-density microelectrode array across hundreds of sites," *Nat Commun,* vol. 4, pp. 2181, 2013.
[28] J. Muller, M. Ballini, P. Livi *et al.*, "High-resolution CMOS MEA platform to study neurons at subcellular, cellular, and network levels," *Lab Chip,* vol. 15, no. 13, pp. 2767-80, Jul 7, 2015.
[29] G. E. Perlin, and K. D.-J. P. s.-. Wise, "Ultra-Compact Integration for Fully-Implantable Neural Microsystems." pp. 228 - 231.
[30] A. M. Sodagar, G. E. Perlin, Y. Yao *et al.*, "An implantable microsystem for wireless multi-channel cortical recording," *Transducers '07 & Eurosensors Xxi, Digest of Technical Papers, Vols 1 and 2*, pp. U38-U39, 2007.
[31] K. D. Wise, A. M. Sodagar, Y. Yao *et al.*, "Microelectrodes, microelectronics, and implantable neural microsystems," *Proceedings of the IEEE,* vol. 96, no. 7, pp. 1184-1202, 2008.
[32] F. Wu, E. Stark, M. Im *et al.*, "An implantable neural probe with monolithically integrated dielectric waveguide and recording electrodes for optogenetics applications," *Journal of Neural Engineering,* vol. 10, no. 5, Oct, 2013.
[33] A. Borna, and K. Najafi, "A Low Power Light Weight Wireless Multichannel Microsystem for Reliable Neural Recording," *IEEE Journal of Solid-*

State Circuits, vol. 49, no. 2, pp. 439-451, Feb, 2014.
[34] K. Seidl, S. Herwik, T. Torfs *et al.*, "CMOS-based high-density silicon microprobe arrays for electronic depth control in intracortical neural recording," *Microelectromechanical Systems, Journal of,* vol. 20, no. 6, pp. 1439-1448, 2011.
[35] P. Ruther, and O. Paul, "New approaches for CMOS-based devices for large-scale neural recording," *Current Opinion in Neurobiology,* vol. 32, pp. 31-37, Jun, 2015.
[36] C. M. Lopez, A. Andrei, S. Mitra *et al.*, "An Implantable 455-Active-Electrode 52-Channel CMOS Neural Probe," *IEEE Journal of Solid-State Circuits,* vol. 49, no. 1, pp. 248-261, Jan, 2014.
[37] C. M. Lopez, S. Mitra, J. Putzeys *et al.*, "A 966-Electrode Neural Probe with 384 Configurable Channels in 0.13 mu m SOI CMOS," *2016 IEEE International Solid-State Circuits Conference*, pp. 392-U550, 2016.
[38] M. Fiscella, K. Farrow, I. L. Jones *et al.*, "Recording from defined populations of retinal ganglion cells using a high-density CMOS-integrated microelectrode array with real-time switchable electrode selection," *Journal of Neuroscience Methods,* vol. 211, no. 1, pp. 103-113, Oct, 2012.
[39] E. Ferrea, A. Maccione, L. Medrihan *et al.*, "Large-scale, high-resolution electrophysiological imaging of field potentials in brain slices with microelectronic multielectrode arrays," *Frontiers in neural circuits,* vol. 6, Nov, 2012.
[40] U. Frey, U. Egert, F. Heer *et al.*, "Microelectronic System for High-Resolution Mapping of Extracellular Electric Fields Applied to Brain Slices," *Biosensors and Bioelectronics,* vol. 24, pp. 2191-2198, 2009.
[41] A. Maccione, M. Garofalo, T. Nieus *et al.*, "Multiscale functional connectivity estimation on low-density neuronal cultures recorded by high-density CMOS Micro Electrode Arrays," *Journal of neuroscience methods,* vol. 207, no. 2, pp. 161-171, Jun, 2012.
[42] F. Franke, M. Fiscella, M. Sevelev *et al.*, "Structures of Neural Correlation and How They Favor Coding," *Neuron,* vol. 89, no. 2, pp. 409-422, Jan, 2016.
[43] K. Yonehara, M. Fiscella, A. Drinnenberg *et al.*, "Congenital Nystagmus Gene FRMD7 Is Necessary for Establishing a Neuronal Circuit Asymmetry for Direction Selectivity," *Neuron,* vol. 89, no. 1, pp. 177-193, Jan, 2016.
[44] M. Radivojevic, D. Jackel, M. Altermatt *et al.*, "Electrical Identification and Selective Microstimulation of Neuronal Compartments Based on Features of Extracellular Action Potentials," *Scientific Reports,* vol. 6, Aug, 2016.
[45] V. Viswam, J. Dragas, A. Shadmani *et al.*, "Multi-Functional Microelectrode Array System Featuring 59,760 Electrodes, 2048 Electrophysiology Channels, Impedance and Neurotransmitter Measurement Units," *2016 IEEE International Solid-State Circuits Conference*, pp. 394-U553, 2016.

CONTACT

*A. Hierlemann, tel: +41 61 387 3150; andreas.hierlemann@bsse.ethz.ch